ResearchGate

See discussions, stats, and author profiles for this publication at: https://www.researchgate.net/publication/276070019

Ultrathin Random Copolymer-Grafted Layers for Block Copolymer Self-Assembly

ARTICLE *in* ACS APPLIED MATERIALS & INTERFACES · MAY 2015

Impact Factor: 6.72 · DOI: 10.1021/acsami.5b02201 · Source: PubMed

CITATIONS
4

READS
36

8 AUTHORS, INCLUDING:

Katia Sparnacci
Amedeo Avogadro University of Eastern Pied…
89 PUBLICATIONS **961** CITATIONS
SEE PROFILE

Valentina Gianotti
Amedeo Avogadro University of Eastern Pied…
69 PUBLICATIONS **845** CITATIONS
SEE PROFILE

Michele Laus
Amedeo Avogadro University of Eastern Pied…
218 PUBLICATIONS **2,315** CITATIONS
SEE PROFILE

Michele Perego
Italian National Research Council
103 PUBLICATIONS **1,263** CITATIONS
SEE PROFILE

Available from: Tommaso Jacopo Giammaria
Retrieved on: 04 February 2016

ACS APPLIED MATERIALS & INTERFACES

Research Article

www.acsami.org

Ultrathin Random Copolymer-Grafted Layers for Block Copolymer Self-Assembly

Katia Sparnacci,[†,‡] Diego Antonioli,[†,‡] Valentina Gianotti,[†,‡] Michele Laus,*[,†,‡] Federico Ferrarese Lupi,[§] Tommaso Jacopo Giammaria,[‡§] Gabriele Seguini,[§] and Michele Perego*[,§]

[†]Dipartimento di Scienze e Innovazione Tecnologica (DISIT), Universitá del Piemonte Orientale "A. Avogadro", Viale T. Michel 11, 15121 Alessandria, Italy

[‡]INSTM, UdR, Alessandria, Italy

[§]Laboratorio MDM, IMM-CNR, Via C. Olivetti 2, 20864 Agrate Brianza, Italy

Supporting Information

ABSTRACT: Hydroxyl-terminated P(S-*r*-MMA) random copolymers (RCPs) with molecular weights (M_n) from 1700 to 69000 and a styrene unit fraction of approximately 61% were grafted onto a silicon oxide surface and subsequently used to study the orientation of nanodomains with respect to the substrate, in cylinder-forming PS-*b*-PMMA block copolymer (BCP) thin films. When the thickness (H) of the grafted layer is greater than 5−6 nm, a perpendicular orientation is always observed because of the efficient decoupling of the BCP film from the polar SiO_2 surface. Conversely, if H is less than 5 nm, the critical thickness of the grafted layer, which allows the neutralization of the substrate and promotion of the perpendicular orientation of the nanodomains in the BCP film, is found to depend on the M_n of the RCP. In particular, when M_n = 1700, a 2.0 nm thick grafted layer is sufficient to promote the perpendicular orientation of the PMMA cylinders in the PS-*b*-PMMA BCP film. A proximity shielding mechanism of the BCP molecules from the polar substrate surface, driven by chain stretching of the grafted RCP molecules, is proposed.

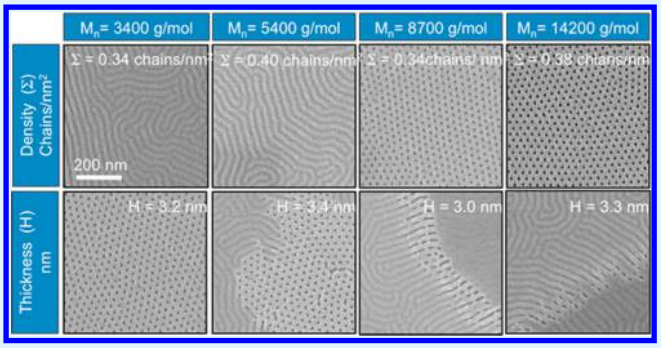

KEYWORDS: *PS-b-PMMA, P(S-r-MMA), self-assembly, rapid thermal processing (RTP), molecular weight*

INTRODUCTION

Nanoscale periodic patterns derived from the self-assembly of block copolymer (BCP) thin films are receiving considerable academic[1−3] and industrial[4,5] attention as precursors for nanolithographic templates featuring small length scales, where traditional photolithographic processes do not allow accessibility. Predetermined periodic structures, characterized by a high degree of registry and regularity in the sub-14 nm regime, can be easily obtained. Control of BCP thin film domain orientation (relative to the plane of the substrate) and alignment (the in-plane directionality) is essential for many applications, in particular for nanoelectronics.[6] Directed self-assembly approaches[4,7,8] (DSA) have been demonstrated to be extremely efficient in controlling the in-plane directionality, guiding the BCP domain structure in the design of basic elements, including lines, spaces, arrays of holes, T-junctions, and jogs.

The domain orientation relative to the plane of the substrate is mainly controlled by the interaction of each block with the substrate and the free surface through wetting energetics and polymer confinement, eventually including commensurability effects that result from the (mis)matching of the BCP periodicity with the film thickness. Preferential wetting of one block of the BCP or the other to the substrate drives the BCP features to be oriented parallel to the plane of the substrate. Spheres and a parallel orientation of cylinders produce patterns similar to perpendicular cylinders and lamellae, respectively. However, the former self-assembled structures exhibit an inherently limited aspect ratio. Consequently, the perpendicular orientation of cylinders or lamellae with respect to the substrate is highly desirable.

The perpendicular orientation of BCP films can be accomplished by several methods such as solvent annealing,[9] application of an electric field,[10] chemical patterns,[11] and surface modification[12−19] to tune the interaction between the BCP and substrate. Among these strategies, the concept of surface modification is by far the more commonly employed. Modified alkyl chlorosilane[12,13] or ethylene glycol[20] self-assembled monolayers (SAMs) on a SiO_2 substrate were used to control the wetting behavior of BCP thin films. Tuning the grafting density of the SAMs resulted in a variation of the surface from preferential to neutral to dewetting.

Received: March 12, 2015
Accepted: May 8, 2015
Published: May 8, 2015

ACS Publications © 2015 American Chemical Society

DOI: 10.1021/acsami.5b02201
ACS Appl. Mater. Interfaces 2015, 7, 10944−10951

The most robust strategy for promoting the perpendicular orientation in BCP thin films was first described by Mansky[14] and relies on the surface modification using end functional poly(A-*r*-B) random copolymers (RCP) chemically grafted to the substrate via the "grafting to" approach. In particular, the use of functional hydroxyl-terminated poly(styrene-*r*-methyl methacrylate) [P(S-*r*-MMA)] RCP is a well-studied approach to inducing the perpendicular orientation in polystyrene-*b*-poly(methyl methacrylate) (PS-*b*-PMMA) BCP. For this class of polymers, at ∼225 °C, the interfacial interactions at the free surface are balanced, thus allowing the perpendicular orientation of domains to be obtained when they are annealed on a neutral substrate surface.[21]

In spite of the relatively low values of the Flory−Huggins interaction parameter χ that limits the resolution of domains to ∼11 nm,[22,23] this class of BCPs represents the current industrial standard for the implementation of novel lithographic approaches based on the integration of self-assembled BCP thin films in conventional photolithographic processes.

The surface neutralization by RCP grafting provides an excellent solution to the problem of surface energy tuning from the perspective of its implementation in a lithographic process for several reasons. First, fine-tuning of the molecular weight (M_n) and composition of the RCP is possible, once a living polymerization technique is employed, thus resulting in very accurate control of the wetting characteristics of the grafted surface.[24−26] In particular, NMP (nitroxide-mediated polymerization)[14] and ARGET-ATRP[27] (activator regenerated by electron transfer−atom transfer polymerization) polymerization using a functionalized starter were quite effective in controlling the composition and M_n of a P(S-*r*-MMA) RCP. Second, the grafting reaction can be accelerated[28,29] by increasing the temperature without problems connected to the vapor pressure of the reactants or the release of aggressive byproducts. Third, the "grafting to" reaction is a self-limiting reaction;[30] thus, it is straightforward to produce a grafted layer featuring homogeneous thickness irrespective of the thickness and homogeneity of the starting spun film (as long as the thickness of the film spun on the surface is several times the ultimate thickness of the grafted layer) or the eventual presence of a temperature gradient along the substrate surface.

In the original paper by Mansky,[14] the RCP leading to the neutral surface was characterized by an M_w of approximately 10000. A layer thickness of ∼6 nm, corresponding approximately to twice the radius of gyration (R_g) of the specific RCP under investigation, was thought to be necessary to decouple the BCP layer from the polar surface, thus promoting the perpendicular orientation of the BCP features. Basically, the same result was obtained[31] with a RCP containing a thermally cross-linkable benzocyclobutene (BCB) monomer to produce an insoluble cross-linked thin film. A minimum thickness of 5.5 nm for the cross-linked P(S-*r*-BCB-*r*-MMA) layer was found to be necessary to mask the underlying substrate and allow the perpendicular orientation of the BCP features.

From a technological point of view, minimization of the thickness of the RCP is important to optimize the fidelity of the pattern transfer. Nonpreferential layers, for the assembly of PS-*b*-PMMA BCPs, that were thinner than 5.5 nm were reported[32] for a different system consisting of poly(styrene-*r*-methyl methacrylate-*r*-glycidyl methacrylate). The effective minimum thickness of the cross-linked layer for the perpendicular alignment of P(S-*b*-MMA) decreased from ∼6 to ∼2 nm as the glycidyl methacrylate concentration in the RCP increased because of the parallel increase in cross-linking efficiency. However, for the latter system, the neutralizing layer thickness is dictated by the spin coating conditions, and consequently, thickness nonhomogeneities are likely to occur in large area samples. In addition, thickness variability in different spin coating depositions could adversely affect the successive workup of the silicon wafer. Finally, a slight decrease in the oxygen plasma etching rate was observed, thus potentially affecting the PS nanotemplate obtained after removal of the PMMA domain by UV exposure followed by washing with acetic acid. Accordingly, in spite of efforts to extend Mansky's concept from end-chain to side-chain grafting reactions,[32,33] the most effective process for surface neutralization still consists of the use of simple end functional RCPs.

In this study, several α-hydroxyl functional P(S-*r*-MMA) RCPs, with different M_n values but equal compositions, are synthesized and subsequently grafted to a SiO_2 surface to tune the surface energy of the substrate and study the interaction of the grafted layer with thin films of asymmetric PS-*b*-PMMA BCP. Substantial differences versus the existing literature in this area can be anticipated, demonstrating the possibility of aggressively scaling down the thickness of the RCP layer that is necessary to effectively neutralize the substrate and to induce the perpendicular orientation of the PMMA cylinders in the PS-*b*-PMMA film.

EXPERIMENTAL SECTION

Materials. 2-Hydroxyethyl(2-bromoisobutyrate) (HEBIB), tris[2-(dimethylamino)ethyl]amine (Me_6TREN), copper(II) bromide ($CuBr_2$), tin(II) 2-ethylhexanoate [$Sn(EH)_2$], and solvents were purchased from Aldrich and used as received. Styrene and methyl methacrylate were purchased from Aldrich and purified by being passed through an inhibitor removal column (Aldrich) before being used. The asymmetric BCP PS-*b*-PMMA, marked B70, with styrene fraction of XS = 0.70 (M_n = 67100, PDI = 1.09, and PMMA syndiotactic rich content of >78%) was purchased from Polymer Source Inc. and used as obtained.

Synthesis of Random Copolymers. The α-hydroxyl ω-Br functional P(S-*r*-MMA) RCPs were marked R*n*, with R standing for random and *n* indicating the M_n of the sample. The lower-M_n samples were synthesized by ARGET-ATRP copolymerization of styrene and methyl methacrylate, whereas the highest-M_n sample was prepared by the ARGET-ATRP extension reaction, described in detail below. This catalytic system, originally introduced by Matyjaszewski[34] for styrene polymerization, allows a significant reduction of the employed copper-based catalyst complex, with respect to the "classical" ATRP system,[35] because of the constant regeneration of the Cu(I) activator species by the reducing agent. The reduction of the amount of metal is important in view of the microelectronic application of these materials.

ARGET-ATRP Copolymerization. The α-hydroxyl ω-Br functional RCPs (R1.7−R19.9) were obtained by ARGET-ATRP of styrene and methyl methacrylate initiated by HEBIB and catalyzed by a $CuBr_2$/Me_6TREN complex in the presence of $Sn(EH)_2$ as the reducing agent. In all samples, the monomer composition (styrene feed molar fraction of 0.70) and the initiator/copper catalyst/ligand/reducing agent molar ratios were kept constant (1/0.02/0.22/0.20 $[HEBIB]_0/[CuBr_2]_0/[Me_6TREN]_0/[Sn(EH)_2]_0$), whereas variations in the reaction time and the monomer/initiator (M/I) molar ratio are allowed to obtain different molar masses. Table 1 lists the synthetic details of the various samples.

As a typical example, the synthetic procedure employed in the synthesis of sample R5.4 is reported in detail. $CuBr_2$ (2.40 mg, 10.3 μmol) and Me_6TREN (2.8 μL, 10.3 μmol) were dissolved in 5.0 mL of degassed anisole and transferred via degassed syringes to a dry Schlenk flask, purged by being flushed with nitrogen. Then, 8.0 mL of degassed styrene (69.8 mmol), 3.3 mL of degassed methyl methacrylate (30.8 mmol), and 75.0 μL of HEBIB (0.50 mmol) were added, and the

DOI: 10.1021/acsami.5b02201
ACS Appl. Mater. Interfaces 2015, 7, 10944−10951

Table 1. Monomer/Initiator Molar Ratios (M/I), Reaction Times (t_R), Conversions (C), Molecular Weights (M_n), Polydispersity Indices (PDI), Styrene Unit Contents (S), and Glass Transition Temperatures (T_g) of the Hydroxyl-Terminated P(S-*r*-MMA) RCPs

sample	M/I	t_R[b] (h)	C (%)	M_n (g mol^{-1})	PDI	S (%)	T_g (°C)
R1.7[a]	30/1	2	11.0	1700	1.19	61.8	69.5
R3.4[a]	100/1	2	18.8	3400	1.20	61.6	71.0
R5.4[a]	200/1	2	13.0	5400	1.17	59.6	77.0
R8.7[a]	200/1	6	31.3	8700	1.19	62.3	84.0
R14.2[a]	200/1	16	52.0	14200	1.25	61.0	97.5
R19.9[a]	250/1	16	55.0	19900	1.29	59.1	100.5
R69.0	700/1[a]	16	28.9	69000	1.19	61.0	103.5

[a][HEBIB]$_0$/[$CuBr_2$]$_0$/[Me_6TREN]$_0$/[$Sn(EH)_2$]$_0$ ratio of 1/0.02/0.22/0.20. [b]T = 90 °C in anisole (0.5 volume equivalents vs monomers).

mixture was degassed by three freeze−thaw cycles. Next, a purged solution of $Sn(EH)_2$ (84.0 μmol) and Me_6TREN (84.0 μmol) in degassed anisole (1.0 mL) was added, and the mixture was sealed under nitrogen. The polymerization was conducted at 90 °C for 2 h. Then, the reaction mixture was cooled to room temperature and the copolymer precipitated into methanol, washed with methanol, purified by precipitation from a THF solution into methanol, isolated by filtration, and then dried under vacuum at room temperature. Monomer conversion was assessed gravimetrically.

ARGET-ATRP Extension. Sample R69.0 was obtained by ARGET-ATRP extension of R14.2, employed as a macroinitiator in the styrene and methyl methacrylate copolymerization; 1.5 g of sample R14.2 (0.10 mmol, M_n = 14200, PDI = 1.25) was dissolved in the monomer mixture (5.7 mL of degassed styrene, 49.8 mmol, and 2.3 mL of degassed methyl methacrylate, 21.5 mmol) and transferred via degassed syringes to a dry Schlenk flask, purged by being flushed with nitrogen. Then, a solution obtained by dissolving 0.91 mg of $CuBr_2$ (4.08 μmol) and 1.5 μL of Me_6TREN (4.8 μmol) in 4.0 mL of degassed anisole was added, and the mixture was degassed by three freeze−thaw cycles. Next, a purged solution of $Sn(EH)_2$ (48.0 μmol) and Me_6TREN (48.0 μmol) in degassed anisole (1.0 mL) was added, and the mixture was sealed under nitrogen. The polymerization was conducted at 90 °C for 16 h. Then, the reaction mixture was cooled to room temperature and diluted with THF (5 mL). The copolymer was precipitated into methanol, washed with methanol, purified by precipitation from a THF solution into methanol, isolated by filtration, and then dried under vacuum at room temperature. Monomer conversion was assessed gravimetrically.

Random Copolymer Characterization. The copolymer composition was evaluated by ^{1}H NMR in $CDCl_3$ employing a Jeol Eclipse ECP300 spectrometer. The SEC analysis was performed on THF solutions of the RCPs using a 590 Waters chromatograph equipped with refractive index and ultraviolet detectors and using a column set consisting of Waters HSPgel HR3 and HR4 columns with a flow rate of 0.6 mL min^{-1}. The column set was calibrated against standard PS samples. Differential scanning calorimetry (DSC) was conducted using a Mettler-Toledo DSC 821 apparatus. Samples of ∼5 mg were employed. The instrument was calibrated with high-purity standards at a rate of 10 °C min^{-1}. Dry nitrogen was used as the purge gas.

Substrate Preparation. Substrates were obtained from (100)-oriented Si wafers with a 50 nm thick thermal SiO_2 layer. Samples with a surface of 1 cm^2 were treated with piranha solution (concentrated H_2SO_4 and 30% H_2O_2 in a 3/1 volume ratio; **Warning:** *piranha solution reacts strongly with organic compounds and should be handled with extreme caution*) at 80 °C for 40 min to remove residual organic material and to increase the density of hydroxyl groups at the surface. The cleaning process of the substrates was completed by rinsing in H_2O, drying in a N_2 flow, and then performing an ultrasonic bath in 2-propanol.

Random Copolymer Grafting. The RCPs (18.0 mg in solution with 2.00 mL of toluene) were spin coated on the substrates for 30 s at 4000 rpm. The samples were then treated using a rapid thermal processing (RTP) apparatus for different time periods at 250 °C in a N_2 atmosphere to promote the grafting reaction. A further ultrasonic bath in toluene was then performed to remove the nongrafted fraction, and the grafted substrate was dried under a N_2 flow. To verify the effective grafting and the presence of unbounded chains, repeated washings in toluene were conducted, and no variation in the initial layer thickness was observed.

Block Copolymer Deposition. The grafted substrates were spin coated with a solution of the B70 BCP (16.0 mg in 2.00 mL of toluene) to obtain polymeric films with a thickness of approximately 30 nm. Finally, to promote the organization of BCPs, the resulting samples were subjected to RTP treatment at 310 °C for 60 s.

Rapid Thermal Processing Treatments. The RTP treatments were performed[29,36,37] in a Jipelec, JetFirst Series system. The process consists of a three-step treatment (a heating ramp, a plateau, and a cooling ramp) in a N_2 atmosphere. In all the thermal treatments, the heating ramp was set at 18 °C s^{-1}.

Film Characterization. The thicknesses of the RCP and BCP films were measured with an M-200U spectroscopic ellipsometer (J. A. Wollam Co. Inc.) using a xenon lamp at a 70° incident angle. The morphological characterization of the self-assembled BCP films was performed by means of scanning electron microscopy (SEM) in a Zeiss Supra 40 system. To improve the contrast of the SEM images, the PMMA phase was selectively removed. The opening of the cylinder patterns was obtained by degrading the PMMA blocks by exposure to UV radiation (5 mW cm^{-2}; λ = 253.7 nm) for 15 min. The samples were treated in oxygen plasma for 60 s at 40 W to remove the PMMA phase and to promote the cross-link of the PS chains. Contact angle measurements were performed using an optical tensiometer (model theta).

RESULTS AND DISCUSSION

Characterization of Random Copolymers. Several α-hydroxyl P(S-*r*-MMA) RCPs were prepared by ARGET-ATRP copolymerization employing the functional initiator HEBIB. The monomer/initiator molar ratio and the reaction time were optimized to obtain functional RCPs with molecular weights ranging from 1700 to 19900 and relatively low polydispersity indices (≤1.3), as evaluated from the SEC curves in Figure 1. Table 1 reports the measured M_n and PDI values of the various samples. As previously reported for the ATRP copolymerization of methyl methacrylate and styrene,[38] the PDI slightly increases with monomer/initiator molar ratio and conversion. Consequently, to prepare high-M_n RCPs, featuring a low PDI, the ARGET-ATRP chain extension procedure was adopted. In

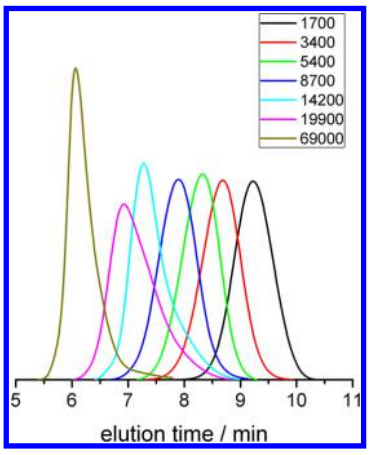

Figure 1. SEC curves of the RCPs prepared by ARGET-ATRP.

DOI: 10.1021/acsami.5b02201
ACS Appl. Mater. Interfaces 2015, 7, 10944−10951

particular, employing R14.2 as the macroinitiator, the R69.0 sample was obtained with an M_n of 69000 and a PDI of 1.19. The corresponding SEC curve is shown in Figure 1.

The RCP composition was evaluated by ^{1}H NMR analysis. In all cases, starting from a constant monomer composition (styrene feed molar fraction of 0.70), RCPs with mole fractions of styrene units ranging from 59.1 to 62.3% were obtained (Table 1), in agreement with the literature for the living radical copolymerization of styrene and methyl methacrylate.[38,39] In the ^{1}H NMR spectra of all samples, the peak at ~2.85 ppm (Figure S1 of the Supporting Information) is present. This signal was ascribed[39] to the -OCH_3 groups of methyl methacrylate units bonded to the styrene units and represents an indication of the formation of P(S-*r*-MMA) RCPs. The composition of the different RCPs is very close to the optimal styrene mole fraction (0.61−0.66) that allows neutralization of the surface preventing preferential wetting of one of the two components of the BCP.[24,25]

The glass transition temperatures (T_g) of the different RCP were determined by DSC and are listed in Table 1. The T_g of the RCPs initially increases as the M_n increases and then levels off, corresponding to molecular weights of approximately 20000.

Grafting Reactions. Figure 2 illustrates the variation of the thickness (H) of the grafted layer for the various RCPs with

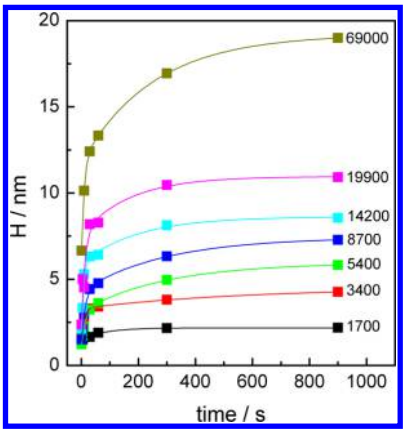

Figure 2. Thicknesses (H) of the grafted layers of the various RCPs as a function of annealing time at 250 °C.

annealing time. All the grafting reactions were performed using a RTP system. The heating ramp for all the experiments was fixed to 18 °C s^{-1}. The grafting experiments were performed at 250 °C, and the transient time to heat the sample from 180 °C (temperature at which the grafting rate is very low) to 250 °C is approximately 4 s. This low transient period allows one to consider performing a majority of the grafting process under isothermal conditions and investigating the process at high temperatures on the time scale of a few seconds.[29] The time evolution of H values is very similar for all the RCP samples. H increases rapidly over a short time period and then very slowly as the time increases, approaching a limiting thickness value H_L, which depends on the M_n of the employed RCP. The corresponding H_L values are listed in Table 2 for the RCPs with different M_n values.

The configurational arrangement of unperturbed RCP chains in a melt corresponds to the random coil configuration with gyration radius R_g defined by eq 1:

Table 2. Radii of Gyration Calculated by eq 1, Limit Layer Thicknesses (H_L), and Corresponding Surface Grafting Densities (Σ_L) Calculated by eq 2 of the Hydroxyl-Terminated P(S-*r*-MMA) RCPs

sample	R_g (nm)	H_L (nm)	Σ_L (chain nm^{-2})
R1.7	1.14	2.2	0.87
R3.4	1.61	4.3	0.85
R5.4	2.03	5.8	0.72
R8.7	2.58	7.3	0.56
R14.2	3.30	8.6	0.41
R19.9	3.90	10.9	0.37
R69.0	7.27	19.0	0.19

$$R_g = \left(N\frac{b^2}{6}\right)^{1/2} \quad (1)$$

where N is the degree of polymerization and b is the average statistical segment length. As the values of b[40] for polystyrene and poly(methyl methacrylate) are 0.68 and 0.69 nm, respectively, the R_g values for the various samples can be estimated and are listed in Table 2. The limiting thickness value (H_L) appears to be somewhat higher than twice the radius of gyration of the corresponding RCP.

These results agree with literature data[41−43] indicating that the limiting grafting thickness increases with the M_n until a value near the critical entanglement M_n is reached. In particular, Iyer et al.[44] demonstrated that for OH-terminated PS chains with M_n values of >100000 a significant reduction in limiting grafting thickness H_L occurs because of the slow diffusion and/or reorientation of the entangled chains. The progressive increase in H_L values in our samples indicates that the M_n values of the RCPs under investigation are below the critical M_n. Starting from the measured H values and assuming that density ρ of the RCP in the grafted film is equal to that in the bulk, surface grafting density Σ for all the grafted samples is determined by eq 2:

$$\Sigma = \frac{H\rho \mathrm{Na}}{M} \quad (2)$$

where H is the layer thickness, Na is Avogadro's number, and M is the molecular weight of the various RCP samples. The trend of Σ for the various RCPs as a function of grafting H at 250 °C is illustrated in Figure 3, whereas the corresponding limiting values Σ_L, corresponding to the maximal thickness, are listed in Table 2.

The Σ at H_L decreases from 0.87 to 0.18 chain nm^{-2} as the M_n increases from R1.7 to R69.0. Considering that, after activation by piranha treatment, the SiO_2 surface is covered[45] by 4.6 ± 0.2 OH groups nm^{-2}, it is clear that the H_L is not related to the amount of functional groups at the SiO_2.

These results suggest that the diffusion of the polymer chains through the already grafted-chain layer is readily feasible until the thickness of the layer is equal to or slightly higher than twice the R_g of the grafted chain. From this point onward, further diffusion and grafting of chains may induce steric constraints causing consistent stretching of the already grafted molecules, in turn resulting in entropic repulsions for nongrafted molecules, reflecting the Kramer's model describing the "grafting to" process from a melt.[46] This consideration is very important for understanding the dynamics of the BCP orientation through interaction with the neutralizing RCP layer, discussed in detail in the next section.

DOI: 10.1021/acsami.5b02201
ACS Appl. Mater. Interfaces 2015, 7, 10944−10951

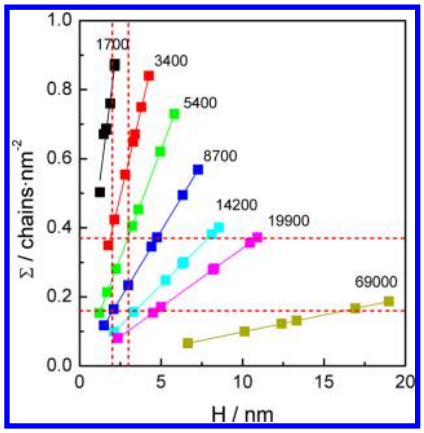

Figure 3. Trend of grafting density Σ for the various RCPs as a function of layer thickness H. The horizontal red lines are drawn at constant grafting densities (Σ) of ∼0.16 and ∼0.37 chain nm^{-2}. The vertical red lines are drawn at the constant layer thicknesses (H) of ∼2 and ∼3 nm.

The entire picture of the curves illustrated in Figure 3 indicates that it is possible to choose samples with the same RCP layer thickness but a different Σ (samples lying along the vertical direction) or samples with the same Σ but a different H (samples lying along the horizontal direction). In this way, the effect of Σ can be decoupled from that of H.

The contact angle of water (θ_w) on the random copolymer brush surfaces was also measured for all the samples. Irrespective of the molar mass and layer thickness, the θ_w value of 82 ± 1° is in good agreement with the literature values.[25] This indicates that the composition of the brush at the surface is identical in all the samples and that the incidence of the bromine end group and of the grafting density is negligible.

Block Copolymer Self-Assembly. Figure 4 shows two sets of SEM images illustrating the evolution of the nanodomain orientation in the BCP films deposited on top of an ∼2 nm (top row) or ∼3 nm (bottom row) thick films of RCP. The M_n of the RCPs ranges from 1700 to 19900. These SEM sequences refer to the dashed vertical lines in Figure 3. The thickness and chemical composition of the neutralizing layers are equivalent, yet the flipping from the perpendicular to parallel orientation of the nanodomains in the BCP film occurs, moving through a mixed orientation showing parallel and perpendicular cylinders simultaneously, with an increase in the M_n of the RCP. The images demonstrate that the critical H necessary to promote the perpendicular orientation of the nanodomains depends on the M_n of the RCP. In particular, in the case of R1.7, the critical H value is ∼2 nm. Conversely, in the case of R3.4, a 2 nm thick RCP film results in a parallel orientation of the nanodomains in the BCP deposited on top of the grafted layer. For the latter RCP, a 3 nm thick layer is necessary to effectively neutralize the substrate and promote the perpendicular orientation of the nanodomains.

It is interesting to note that, as the M_n increases, the RCP Σ decreases. The 2 nm thick film, corresponding to the RCP with the lowest M_n (R1.7), exhibits a very high grafting density of 0.87 chain nm^{-2}. Conversely, in the case of R19.9, the grafting density decreases to 0.08 chain nm^{-2}. These data apparently suggest a correlation between the RCP Σ and the orientation of the nanodomains in the BCP films.

From this perspective, Figure 5 reports a collection of representative SEM images showing the orientation of the nanodomains in the BCP layer deposited on top of RCP films at constant grafting densities of ∼0.16 chain nm^{-2} (top row) and ∼0.37 chain nm^{-2} (bottom row), corresponding to the dashed horizontal lines in Figure 3. The M_n of the RCP varies from 3400 to 69000. The BCP nanodomain orientation changes from parallel to perpendicular, moving through a mixed orientation as the M_n of the RCP increases. The mixed morphology is clearly detectable in the case of RCP R19.9 at a Σ of 0.15 chain nm^{-2}. The images demonstrate that effective neutralization of the substrate can be achieved even in grafted films with a Σ of ∼0.15 chain nm^{-2}, i.e., with a very low Σ, provided that the M_n of the RCP is sufficiently high (69000). Similarly, in the case in which Σ ∼ 0.37 chain nm^{-2}, a perpendicular organization of the BCP nanodomains is observed for M_n values of ≥8700. It is worth noting that, for a fixed value of Σ, the thickness of the RCP layer progressively expands as the M_n of the RCP increases.

The described phenomenology indicates that the surface neutralization effect cannot be ascribed to simple considerations of the H or Σ of the RCP layer and that a more sophisticated mechanism is involved. Figure 6 provides a general overview of the orientation of nanodomains in the BCP thin film for the various RCPs. The thicknesses of the RCP film corresponding to the perpendicular orientation of the nanodomains are colored green. Conversely, red is used to indicate the mixed or parallel orientation of the cylinders. The intrinsic discreteness of the thickness values obtained from the grafting process is reflected by the presence of small empty spaces

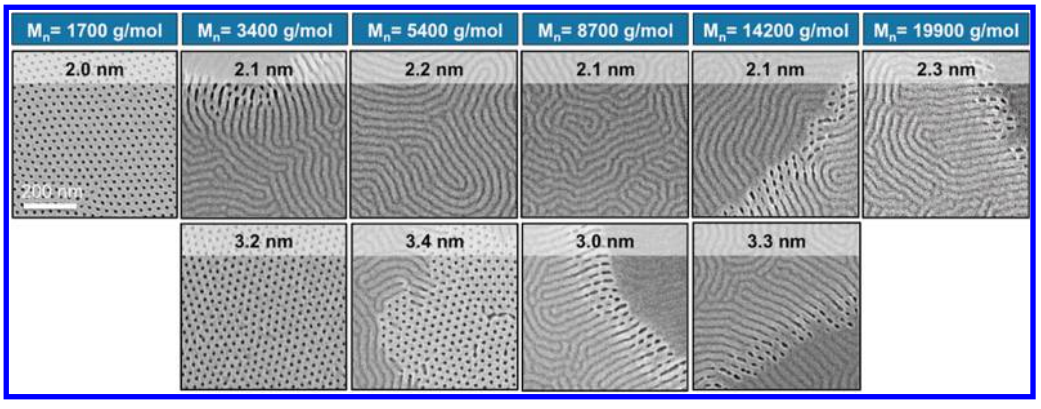

Figure 4. SEM plan view images illustrating the evolution of the nanodomain orientation in BCP films deposited on top of an ∼2 nm (top) and ∼3 nm (bottom) thick RCP layer with different molecular weights.

DOI: 10.1021/acsami.5b02201
ACS Appl. Mater. Interfaces 2015, 7, 10944−10951

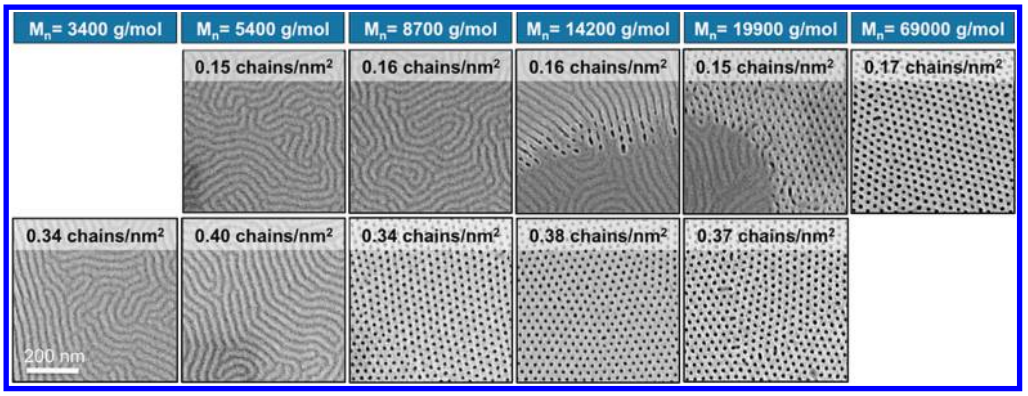

Figure 5. SEM plan view images illustrating the evolution of the nanodomain orientation in BCP films deposited on top of RCP layers with Σ values of ∼0.15 chain nm^{-2} (top) and ∼0.37 chain nm^{-2} (bottom).

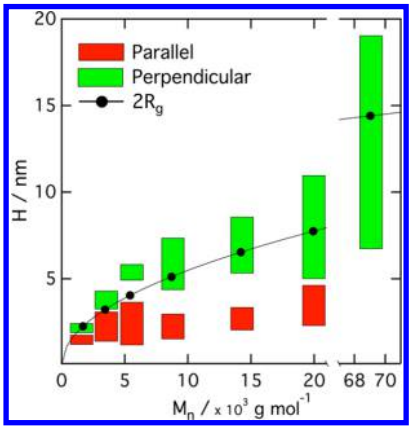

Figure 6. Thickness windows of the RCP layers corresponding to the perpendicular (green) and parallel (red) orientation of the nanodomains in the BCP film deposited on top of the grafted layer as a function of the RCP molecular weight. The black dots indicate the thickness values corresponding to $2R_g$ for each M_n value.

between the red bars corresponding to the parallel or mixed orientation and the green bar corresponding to the perpendicular orientation. The black line corresponds to twice the R_g value of the different RCPs. The minimal H required to effectively neutralize the substrate progressively shifts toward higher values with an increase in the M_n of the RCP with a leveling off around 5−6 nm, in agreement with the literature.[14] It is apparent that, for RCPs with low M_n values (i.e., <15000), the limiting H for the perpendicular organization of the BCP features depends on the M_n and closely parallels the $2R_g$ value of the corresponding RCP.

The overall picture of the data indicates that we can account for the surface neutralization by considering two distinct regimes. When the H of the grafted layer is equal to or greater than 5−6 nm, the distance between the polar groups on the SiO_2 surface and the BCP layer is large enough to prevent any direct interaction, irrespective of the density of the grafted layer. Consequently, in this regime, the key parameter that determines the surface neutrality is simply the H of the grafted layer that spatially decouples the BCP film from the SiO_2 substrate. On the other hand, when the H of the grafted layer is <5 nm, the effective neutralization of the substrate depends on a critical interplay between the H and Σ that reflects the peculiar configurational arrangement of the grafted chains.

A possible interpretation could be suggested considering the physics of the grafting process discussed in the previous section. During the first stage of the grafting process, the grafting of molecules to the substrate is limited by classical diffusion of polymer chains. In the case presented here, because grafting occurs from melting, the polymer chains are already in place and they need to reorient only within the first monolayer to allow the reaction of their terminal group with the functionalities on the substrate surface. When the H of the grafted layer approaches $2R_g$, the grafting process decelerates because the configuration of the grafted molecules approximates the shape of the random coil. Under this condition, the attachment of new macromolecules requires the grafted chains to stretch to accommodate them. Consequently, the incoming macromolecules need to overcome the potential barrier determined by the entropy loss associated with grafted-chain stretching.[44,46]

We suggest that the same proximity shielding mechanism, caused by chain stretching of the grafted molecules, is operating when the BCP is deposited on top of the grafted film. In particular, when the H of the grafted film is less than $2R_g$, the BCP chains can penetrate the grafted layer and interact with the underlying substrate, resulting in the parallel or mixed orientation of the nanodomains. Conversely, when the H of the grafted layer approaches $2R_g$, the diffusion of the BCP chains would induce steric constraints causing stretching of the already grafted molecules, thus in turn resulting in entropic repulsions. This entropic repulsion produces an effective shielding of the underlying SiO_2 substrate, preventing interactions with the BCP film. Under this condition, an effectively neutral surface is obtained, leading to the perpendicular organization of the BCP features.

From a technological point of view, these results indicate that it is possible to significantly reduce the critical thickness of the RCP that effectively neutralizes the substrate and consequently promotes the perpendicular orientation of the nanodomains by using RCP with a low M_n. In a recent paper, it was demonstrated that the choice of the RCP is crucial for the implementation of a disposable polymeric mask with well-controlled dimensions.[22,23] The average pore diameter in the final polymeric film deposited on the RCP depends on the duration of the O_2 plasma treatment that is necessary to remove the RCP from the bottom of the pores and completely open the mask.[47] In this regard, a thin RCP layer would result in a relatively short O_2 plasma exposure and consequently a minimization of the pore enlargement caused by the isotropic etching.

DOI: 10.1021/acsami.5b02201
ACS Appl. Mater. Interfaces 2015, 7, 10944−10951

CONCLUSIONS

The neutralization of a SiO_2 surface was studied using hydroxyl-terminated P(S-*r*-MMA) RCPs, with different M_n values but equal compositions. The overall picture of the data indicates that the orientation of the nanodomains in the BCP thin film deposited on top of the RCP-grafted layer results from a quite complex balance among several parameters and involves two distinct regimes. For thick RCP films ($H \geq 5$ nm), the interaction with the underlying substrate is inhibited by the limited interpenetration between the RCP and the BCPs and a perpendicular orientation is obtained. However, when the H is <5 nm, a critical interplay between the H and Σ of the RCP is observed. The critical thickness necessary to promote the perpendicular orientation of the cylinders in the BCP thin film changes as a function of the M_n of the RCP. An effective neutralization is observed for a specific M_n value when H nears $2R_g$. For this H value, the configuration of the grafted RCP molecules closely resembles the random coil and the diffusion of the BCP into the grafted layer is counteracted by the entropy loss associated with the stretching of the grafted chains necessary to accommodate the BCP molecules. Within this regime, 2 nm thick films of RCPs with an M_n of 1700 ($2R_g$ = 2.1 nm) are sufficient to promote the perpendicular orientation of the PMMA cylinders in the PS-*b*-PMMA BCP film. From a technological point of view, minimization of the thickness of the RCP allows optimization of pattern transfer fidelity.

ASSOCIATED CONTENT

Supporting Information

Copolymer composition evaluated by ^1H NMR in $CDCl_3$ and spectra of sample R1.7 (M_n = 1700; PDI = 1.19). The Supporting Information is available free of charge on the ACS Publications website at DOI: 10.1021/acsami.5b02201.

AUTHOR INFORMATION

Corresponding Authors

*E-mail: michele.laus@mfn.unipmn.it.
*E-mail: michele.perego@mdm.imm.cnr.it.

Notes

The authors declare no competing financial interest.

ACKNOWLEDGMENTS

This research activity was partially funded by the European Metrology Research Programme (EMRP), Project new01-TReND. The EMRP is jointly funded by the EMRP participating countries within EURAMET and the European Union. Partial financial support by PRIN 2010-2011 "Materiali Polimerici Nanostrutturati con Strutture Molecolari e Crystalline Mirate" is acknowledged. Patent protection related to this work is pending.

REFERENCES

(1) Hamley, I. W. Ordering in Thin Films of Block Copolymers: Fundamentals to Potential Applications. *Prog. Polym. Sci.* **2009**, *34*, 1161−1210.
(2) Darling, S. B. Directing the Self-Assembly of Block Copolymers. *Prog. Polym. Sci.* **2007**, *32*, 1152−1204.
(3) Koo, K.; Ahn, H.; Kim, S. W.; Ryu, D. Y.; Russell, T. P. Directed Self-Assembly of Block Copolymers in the Extreme: Guiding Microdomains from the Small to the Large. *Soft Matter* **2013**, *9*, 9059−9071.
(4) Herr, D. J. C. Directed Block Copolymer Self-Assembly for Nanoelectronics Fabrication. *J. Mater. Res.* **2011**, *26*, 122−139.
(5) Stoykovich, M. P.; Kang, H.; Daoulas, K. C.; Liu, G.; Liu, C.; de Pablo, J. J.; Müller, M.; Nealey, P. F. Directed Self-Assembly of Block Copolymers for Nanolithography: Fabrication of Isolated Features and Essential Integrated Circuit Geometries. *ACS Nano* **2007**, *1*, 168−175.
(6) Bates, C. M.; Maher, M. J.; Janes, D. W.; Ellison, C. J.; Willson, C. G. Block Copolymer Lithography. *Macromolecules* **2014**, *47*, 2−12.
(7) Kim, H. C.; Park, S. M.; Hinsberg, W. D. Block Copolymer Based Nanostructures: Materials, Processes, and Applications to Electronics. *Chem. Rev.* **2010**, *110*, 146−177.
(8) Li, M.; Ober, C. K. Block Copolymer Patterns and Templates. *Mater. Today* **2006**, *9*, 30−39.
(9) Kim, S. H.; Misner, M. J.; Xu, T.; Kimura, M.; Russell, T. P. Highly Oriented and Ordered Arrays from Block Copolymers via Solvent Evaporation. *Adv. Mater. (Weinheim, Ger.)* **2004**, *16*, 226−231.
(10) Thurn-Albrecht, T.; Schotter, J.; Kastle, C. A.; Emley, N.; Shibauchi, T.; Krusin-Elbaum, L.; Guarini, K.; Black, C. T.; Tuominen, M. T.; Russell, T. P. Ultra High-Density Nanowire Arrays Grown in Self-Assembled Diblock Copolymer Templates. *Science* **2000**, *290*, 2126−2129.
(11) Kim, S. O.; Solak, H. H.; Stoykovich, M. P.; Ferrier, N. J.; de Pablo, J. J.; Nealey, P. F. Epitaxial Self-Assembly of Block Copolymers on Lithographically Defined Nanopatterned Substrates. *Nature* **2003**, *424*, 411−414.
(12) Peters, R. D.; Yang, X. M.; Kim, T. K.; Nealey, P. F. Wetting Behavior of Block Copolymers on Self-Assembled Films of Alkylchlorosiloxanes: Effect of Grafting Density. *Langmuir* **2000**, *16*, 9620−9626.
(13) Peters, R. D.; Yang, X. M.; Kim, T. K.; Sohn, B. H.; Nealey, P. F. Using Self-Assembled Monolayers Exposed to X-rays to Control the Wetting Behavior of Thin Films of Diblock Copolymers. *Langmuir* **2000**, *16*, 4625−4631.
(14) Mansky, P.; Liu, Y.; Huang, E.; Russell, T. P.; Hawker, C. Controlling Polymer-Surface Interactions with Random Copolymer Brushes. *Science* **1997**, *275*, 1458−1460.
(15) Ryu, D. Y.; Shin, K.; Drockenmuller, E.; Hawker, C. J.; Russell, T. P. A Generalized Approach to the Modification of Solid Surfaces. *Science* **2005**, *308*, 236−239.
(16) Ji, S.; Liu, C. C.; Son, J. G.; Gotrik, K.; Craig, G. S. W.; Gopalan, P.; Himpsel, F. J.; Char, K.; Nealey, P. F. Generalization of the Use of Random Copolymers To Control the Wetting Behavior of Block Copolymer Films. *Macromolecules* **2008**, *41*, 9098−9103.
(17) Suh, H. S.; Kang, H.; Liu, C. C.; Nealey, P. F.; Char, K. Orientation of Block Copolymer Resists on Interlayer Dielectrics with Tunable Surface Energy. *Macromolecules* **2010**, *43*, 461−466.
(18) Bang, J.; Bae, J.; Löwenhielm, P.; Spiessberger, C.; Given-Beck, S. A.; Russell, T. P.; Hawker, C. J. Facile Routes to Patterned Surface Neutralization Layers for Block Copolymer Lithography. *Adv. Mater. (Weinheim, Ger.)* **2007**, *19*, 4552−4557.
(19) Shengxiang, J.; Liu, G.; Zheng, F.; Craig, G. S. W.; Himpsel, F. J.; Nealey, P. F. Preparation of Neutral Wetting Brushes for Block Copolymer Films from Homopolymer Blends. *Adv. Mater. (Weinheim, Ger.)* **2008**, *20*, 3054−3060.
(20) Borah, D.; Ozmen, M.; Rasappa, S.; Shaw, M. T.; Holmes, J. D.; Morris, M. Molecularly Functionalized Silicon Substrates for Orientation Control of the Microphase Separation of PS-b-PMMA and PS-b-PDMS Block Copolymer Systems. *Langmuir* **2013**, *29*, 2809−2820.
(21) Mansky, P.; Russell, T. P.; Hawker, C. J.; Mays, J.; Cook, D. C.; Satija, S. K. Interfacial Segregation in Disordered Block Copolymers: Effect of Tunable Surface Potentials. *Phys. Rev. Lett.* **1997**, *79*, 237−240.
(22) Seguini, G.; Giammaria, T. J.; Ferrarese Lupi, F.; Sparnacci, K.; Antonioli, D.; Gianotti, V.; Vita, F.; Placentino, I. F.; Hilhorst, J.; Ferrero, C.; Francescangeli, O.; Laus, M.; Perego, M. Thermally Induced Self-Assembly of Cylindrical Nanodomains in Low Molecular Weight PS-b-PMMA Thin Films. *Nanotechnology* **2014**, *25*, 045301.
(23) Ferrarese Lupi, F.; Giammaria, T. J.; Seguini, G.; Vita, F.; Francescangeli, O.; Sparnacci, K.; Antonioli, D.; Gianotti, V.; Laus, M.; Perego, M. Fine Tuning of Lithographic Masks through Thin Films of

DOI: 10.1021/acsami.5b02201
ACS Appl. Mater. Interfaces 2015, 7, 10944−10951

PS-b-PMMA with Different Molar Mass by Rapid Thermal Processing. *ACS Appl. Mater. Interfaces* **2014**, *6*, 7180−7188.
(24) Han, E.; Stuen, K. O.; La, Y. H.; Nealey, P. F.; Gopalan, P. Effect of Composition of Substrate-Modifying Random Copolymers on the Orientation of Symmetric and Asymmetric Diblock Copolymer Domains. *Macromolecules* **2008**, *41*, 9090−9097.
(25) Ham, S.; Shin, C.; Kim, E.; Ryu, D. Y.; Jeong, U.; Russell, T. P.; Hawker, C. J. Microdomain Orientation of PS-b-PMMA by Controlled Interfacial Interactions. *Macromolecules* **2008**, *41*, 6431−6437.
(26) Han, E.; Stuen, K. O.; Leolukman, M.; Liu, C. C.; Nealey, P. F.; Gopalan, P. Perpendicular Orientation of Domains in Cylinder-Forming Block Copolymer Thick Films by Controlled Interfacial Interactions. *Macromolecules* **2009**, *42*, 4896−4901.
(27) Sparnacci, K.; Antonioli, D.; Gianotti, V.; Laus, M.; Zuccheri, G.; Ferrarese Lupi, F.; Giammaria, T. J.; Seguini, G.; Ceresoli, M.; Perego, M. Thermal Stability of Functional P(S-r-MMA) Random Copolymers for Nanolithographic Applications. *ACS Appl. Mater. Interfaces* **2015**, *7*, 3920−3930.
(28) Liu, C. C.; Thode, C. J.; Rincon Delgadillo, P. A.; Craig, G. S. W.; Nealey, P. F.; Gronheid, R. Towards an All-Track 300 mm Process for Directed Self-assembly. *J. Vac. Sci. Technol., B: Nanotechnol. Microelectron.: Mater., Process., Meas., Phenom.* **2011**, *29*, 06F203.
(29) Ferrarese Lupi, F.; Giammaria, T. J.; Seguini, G.; Ceresoli, M.; Perego, M.; Antonioli, D.; Gianotti, V.; Sparnacci, K.; Laus, M. Flash Grafting of Functional Random Copolymers for Surface Neutralization. *J. Mater. Chem. C* **2014**, *2*, 4909−4917.
(30) Zhao, B.; Brittain, W. J. Polymer Brushes: Surface-Immobilized Macromolecules. *Prog. Polym. Sci.* **2000**, *25*, 677−710.
(31) Ryu, D. Y.; Wang, J. Y.; Lavery, K. A.; Drockenmuller, E.; Satija, S. K.; Hawker, C. J.; Russell, T. P. Surface Modification with Cross-Linked Random Copolymers: Minimum Effective Thickness. *Macromolecules* **2007**, *40*, 4296−4300.
(32) Han, E.; Gopalan, P. Cross-Linked Random Copolymer Mats as Ultrathin Nonpreferential Layers for Block Copolymer Self-Assembly. *Langmuir* **2010**, *26*, 1311−1315.
(33) In, I.; La, Y. H.; Park, S. M.; Nealey, P. F.; Gopalan, P. Side-Chain-Grafted Random Copolymer Brushes as Neutral Surfaces for Controlling the Orientation of Block Copolymer Microdomains in Thin Films. *Langmuir* **2006**, *22*, 7855−7860.
(34) Jakubowski, W.; Min, K.; Matyjaszewski, K. Activators Regenerated by Electron Transfer for Atom Transfer Radical Polymerization of Styrene. *Macromolecules* **2006**, *39*, 39−45.
(35) Matyjaszewski, K.; Xia, J. Atom Transfer Radical Polymerization. *Chem. Rev.* **2001**, *101*, 2921−2990.
(36) Ferrarese Lupi, F.; Giammaria, T. J.; Ceresoli, M.; Seguini, G.; Sparnacci, K.; Antonioli, D.; Gianotti, V.; Laus, M.; Perego, M. Rapid Thermal Processing of Self-Assembling Block Copolymer Thin Films. *Nanotechnology* **2013**, *24*, 315601.
(37) Ceresoli, M.; Ferrarese Lupi, F.; Seguini, G.; Sparnacci, K.; Gianotti, V.; Antonioli, D.; Laus, M.; Boarino, L.; Perego, M. Evolution of Lateral Ordering in Symmetric Block Copolymer Thin Films upon Rapid Thermal Processing. *Nanotechnology* **2014**, *25*, 275601.
(38) Semsarzadeh, M. A.; Abdollahi, M. Kinetic Study of Atom Transfer Radical Homo- and Copolymerization of Styrene and Methyl Methacrylate Initiated with Trichloromethyl-Terminated Poly(Vinyl Acetate) Macroinitiator. *Polymer* **2008**, *49*, 3060−3069.
(39) Gao, J.; Zhang, Z.; Zhou, N.; Cheng, Z.; Zhu, J.; Zhu, X. Copper(0)-Mediated Living Radical Copolymerization of Styrene and Methyl Methacrylate at Ambient Temperature. *Macromolecules* **2011**, *44*, 3227−3232.
(40) Ballard, D. G. H.; Wignall, G. D.; Schelten, J. Measurement of Molecular Dimensions of Polystyrene Chains in the Bulk Polymer by Low Angle Neutron Diffraction. *Eur. Polym. J.* **1973**, *9*, 965−969.
(41) Iyer, K. S.; Luzinov, I. Effect of Macromolecular Anchoring Layer Thickness and Molecular Weight on Polymer Grafting. *Macromolecules* **2004**, *37*, 9538−9545.
(42) Zdyrko, B.; Swaminatha Iyer, K.; Luzinov, I. Macromolecular Anchoring Layers for Polymer Grafting: Comparative Study. *Polymer* **2006**, *47*, 272−279.
(43) Ostaci, R. V.; Damiron, D.; Al Akhrass, S.; Grohens, Y.; Drockenmuller, E. Poly(Ethylene Glycol) Brushes Grafted to Silicon Substrates by Click Chemistry: Influence of PEG Chain Length, Concentration in the Grafting Solution and Reaction Time. *Polym. Chem.* **2011**, *2*, 348.
(44) Iyer, K. S.; Zdyrko, B.; Malz, H.; Pionteck, J.; Luzinov, I. Polystyrene Layers Grafted to Macromolecular Anchoring Layer. *Macromolecules* **2003**, *36*, 6519−6526.
(45) Masteika, V.; Kowal, J.; Braithwaite, N. S. J.; Rogers, T. A Review of Hydrophilic Silicon Wafer Bonding. *ECS J. Solid State Sci. Technol.* **2014**, *3*, Q42−Q54.
(46) Kramer, E. J. Grafting Kinetics of End-Functional Polymers at Melt Interfaces. *Isr. J. Chem.* **1995**, *35*, 49−54.
(47) Andreozzi, A.; Poliani, E.; Seguini, G.; Perego, M. The Effect of Random Copolymer on the Characteristic Dimensions of Cylinder-Forming PS-b-PMMA Thin Films. *Nanotechnology* **2011**, *22*, 185304.

DOI: 10.1021/acsami.5b02201
ACS Appl. Mater. Interfaces 2015, 7, 10944−10951